Available online at www.sciencedirect.com
ScienceDirect
Trans. Nonferrous Met. Soc. China 26(2016) 414−422
Transactions of Nonferrous Metals Society of China
www.tnmsc.cn

Deformation behavior of Ti−5Al−2Sn−2Zr−4Mo−4Cr alloy with two initial microstructures during hot working

Jiao LUO, Lian LI, Miao-quan LI

School of Materials Science and Engineering, Northwestern Polytechnical University, Xi’an 710072, China

Received 5 March 2015; accepted 27 July 2015

Abstract: The effects of initial microstructure on the flow stress, strain rate sensitivity (m), strain hardening exponent (n), apparent activation energy (Q) for deformation of Ti−5Al−2Sn−2Zr−4Mo−4Cr alloy were investigated using isothermal compression tests. Results show that the alloy with Widmanstätten alpha plates shows a higher peak stress and flow softening. Additionally, the alloy with equiaxed primary alpha exhibits an early yield drop at or above 810 °C and at strain rates of 0.1−5.0 s^{-1}. In the strain range of 0.5−0.7, m of the alloy with equiaxed primary alpha is found to be larger at 0.01 s^{-1} and lower deformation temperatures. This phenomenon could be reasonably explained based on the microstructure evolution. The strain has a significant effect on n of the alloy with Widmanstätten alpha plates, which is attributed to platelet bending/kinking and dynamic globularization of α phase. In the strain range of 0.15−0.55, Q of the alloy with Widmanstätten alpha plates is larger.

Key words: titanium alloy; isothermal compression; flow stress; microstructure evolution; dynamic globularization

1 Introduction

The mechanical properties of material are closely related to its final microstructure features (i.e., grain size, volume fraction of phase, phase morphology) [1]. The final microstructure is dependent on the various microstructure characteristics inherited from the initial microstructure morphology and processing parameters during hot forming. Therefore, an increased understanding of the relationship among the initial microstructure morphology, processing and microstructure evolution is particularly critical for sustaining further improvements in performance and reliability of material. Recent research has reported the effects of the initial microstructure, deformation temperature and strain rate on the deformation behavior and microstructure evolution during hot forging of AZ91 magnesium alloy [2], 2219 aluminum alloy [3], 45 steel [4], Ti−10V−2Fe−3Al titanium alloy [5,6]. In particular, a significant difference of flow softening between different initial microstructures was observed in the shapes of the flow stress−strain curves, which can be reasonably explained by microstructure evolution. For instance, JACKSON et al [6] noted that near-β alloy Ti−10V−2Fe−3Al with a high aspect ratio of Widmanstätten α platelets produced more significant flow softening than that with globular primary α, which was attributed to the breaking up of the Widmanstätten α platelets. However, it is not easy to determine the concrete effect on the deformation behavior because various microstructure characteristics are interdependent.

Ti−5Al−2Sn−2Zr−4Mo−4Cr alloy (a “β-rich” α+β titanium alloy) is characterized by high strength, excellent corrosion resistance, superior fracture toughness and significant hardenability, which makes it an ideal material in the aviation and aerospace industries. In the past several years, the deformation behavior of this alloy has been examined extensively due to the benefits of its extended formability [7−9]. However, the effect of the initial microstructure on the deformation behavior of the alloy has not been reported. Therefore, this study aims to clarify the deformation characteristics of a “β-rich” α+β titanium alloy in the α+β two-phase region with different initial microstructures.

In this study, two initial microstructures are firstly obtained by changing the heating treatment processes. Secondly, the effects of the initial microstructure

Foundation item: Projects (51205318, 51275416) supported by the National Natural Science Foundation of China; Project (2012KJ02002) supported by the Innovation Fund of Science and Technology in Northwestern Polytechnical University, China
Corresponding author: Jiao LUO; Tel: +86-29-88460328; E-mail: luojiao@nwpu.edu.cn
DOI: 10.1016/S1003-6326(16)64130-4

and processing parameters (i.e., deformation temperature, strain rate and strain) on the flow stress, the strain rate sensitivity (m), the strain hardening exponent (n) and the apparent activation energy for deformation (Q) were analyzed and detail explanation is given with the help of the microstructure observations during isothermal compression of Ti−5Al−2Sn−2Zr−4Mo−4Cr alloy.

2 Experimental

2.1 Material

In this study, a piece of bar stock alloy with a diameter of 50.0 mm was used. The chemical composition (mass fraction, %) of this alloy was as follows: 5.12 Al, 2.03 Sn, 2.10 Zr, 4.04 Mo, 3.94 Cr, 0.10 Fe, 0.012 C, 0.007 N, 0.007 H, and 0.12 O with balance Ti. The β transus temperature for this alloy was determined to be 905 °C by a technique involving heat treatment followed by optical metallography [10]. A three-stage heat treatment (840 °C, 1 h + air cooling + 800 °C, 4 h + water quenching + 630 °C, 8 h + air cooling) was performed on the alloy, and a SEM image of the alloy with equiaxed microstructure (AB) is shown in Fig. 1. The microstructure AB consists of equiaxed primary α phase (grain size ~3.29 μm) and elongated primary α phase (feret ratio ~5.52) and a small amount of β-transformed phase (grain size ~2.37 μm). The volume fraction of α phase for the alloy was examined using quantitative metallography image analysis software and was found to be near 34.9%.

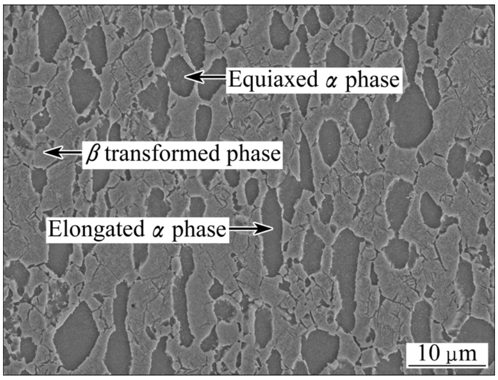

Fig. 1 SEM image of Ti−5Al−2Sn−2Zr−4Mo−4Cr alloy at room temperature (microstructure AB)

To obtain a transformed microstructure (B), this alloy underwent a heat treatment of 910 °C for 20 min with a furnace cool to room temperature. SEM image of the transformed Ti−5Al−2Sn−2Zr−4Mo−4Cr microstructure at room temperature is shown in Fig. 2. The lamellar microstructure (B) has a prior-β grain size of approximately 260 μm. The β grains contain a high volume fraction of Widmanstätten α plates with a high feret ratio. The thickness of α lamellae in microstructure B is 0.24 μm.

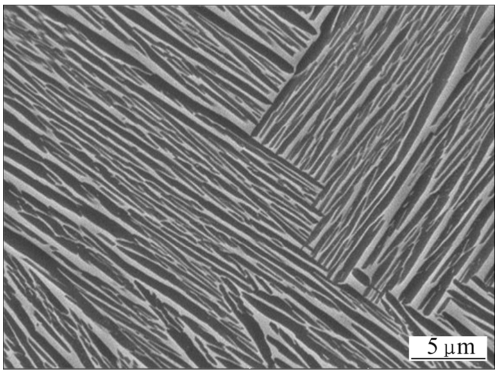

Fig. 2 SEM image of transformed Ti−5Al−2Sn−2Zr−4Mo−4Cr microstructure at room temperature (microstructure B)

2.2 Procedures

Cylindrical compression specimens were 8.0 mm in diameter and 12.0 mm in height. A series of isothermal compression tests of the alloy with microstructures AB and B were conducted on a Gleeble−1500 simulator at deformation temperatures of 770, 790, 810, 830, 850 and 870 °C, strain rates of 0.01, 0.1, 1.0 and 5.0 s^{-1}, and strains of 0.5, 0.7 and 0.9. The specimens were heated and held for 5 min at the given deformation temperature to establish a uniform temperature throughout the specimens. Flow stress−strain curves were recorded automatically during isothermal compression. After isothermal compression, the specimens were cooled in air to room temperature, and the specimens were axially sectioned, electropolished and chemically etched in a solution of 10 mL HF, 15 mL HNO_3 and 75 mL H_2O. The grain size and volume fraction of each phase were measured using quantitative metallography image analysis software (Image-Pro Plus 6.0), and the grain size and volume fraction were calculated by the average value of sixteen visual fields.

3 Results and discussion

3.1 Flow stress

Figure 3 shows the flow stress−strain curves of Ti−5Al−2Sn−2Zr−4Mo−4Cr alloy with two initial microstructures. It is observed that the overall shapes of the flow curves are dependent on the deformation temperature, strain rate and initial microstructure. At a deformation temperature of 770 °C (Fig. 3(a)), the flow stress of two initial microstructures (i.e., microstructures AB and B) firstly increases with increasing strain, reaches a peak value at a critical strain, and then gradually decreases to a steady value. There is a smooth transition from yield to steady state at a deformation temperature of 770 °C, irrespective of the strain rate and initial microstructure. However, an early yield drop of the alloy with microstructure AB is observed at or above 810 °C and at higher strain rates ranging from 0.1 to

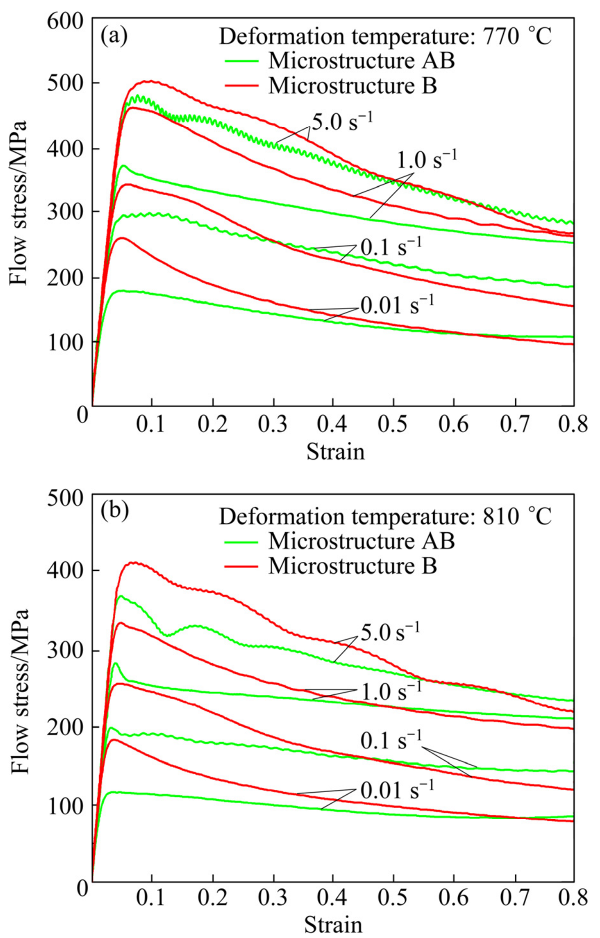

Fig. 3 Flow stress−strain curves of Ti−5Al−2Sn−2Zr−4Mo−4Cr alloy with different microstructures [11]

5.0 s^{-1}. This is not remarkable for the alloy with microstructure AB at lower strain rate (0.01 s^{-1}) and microstructure B, as shown in Fig. 3(b). The occurrence of early yield drop is possibly attributed to the fact that high strain rates promote less time for recovery process and higher local stress concentrations due to dislocation pile-up, so a sufficiently highly applied stress is required to loosen dislocations from their pinning points. Once the dislocations get rid of their pinning locations, dislocation motion and grain boundary sliding for microstructure AB are easier, which will lead to a sharp decrease of flow stress. Thus, the flow stress of the alloy with microstructure AB exhibits an early yield drop at or above 810 °C and at higher strain rates ranging from 0.1 to 5.0 s^{-1}. In the case of microstructure B, the final microstructure exhibits no significant evidence of platelet bending and globularization when the strain is up to 0.5. Only a dynamic recovery process is considered to produce softening during early deformation, which will be supported by the microstructure characterization discussed later in Section 3.2. So, an abrupt decrease in the flow stress during initial strain is not observed for microstructure B. As the deformation degree continually increases, the bucking and break-up of α plates in microstructure B will also be responsible for flow softening. The similar yield drop phenomenon for Ti−10V−2Fe−3Al alloy was also reported [5]. WANJARA et al [12] noted that the occurrence of yielding phenomenon in IMI834 could be rationalized within existing static and/or dynamic deformation theories.

It is also observed that the initial microstructure significantly affects the peak stress of the alloy. The peak stress of microstructure B is higher than that of microstructure AB at a given deformation temperature and strain rate because grain boundaries act as obstacles to dislocation motion; dislocations are hindered and piled up at grain boundaries during early deformation (i.e., before critical strain). The alloy with microstructure B has more grain boundaries than that with microstructure AB, leading to the need for a higher applied stress to loosen dislocations from their pinned locations. Moreover, Widmanstätten α plates and grain boundary α in microstructure B constrain the deformation of the soft β phase; this also results in higher flow stress. Therefore, these two aspects finally produce that a peak stress of microstructure B is higher than that of microstructure AB. Similarly, WEISS and SEMIATIN [13] observed that commercial pure (CP) titanium grade 2 with an acicular starting microstructure exhibited higher flow stress during a high temperature deformation. CP titanium grade 3 with an equiaxed starting microstructure showed lower flow stress and work hardening. JACKSON et al [6] also reported that Ti−10V−2Fe−3Al alloy with high aspect ratios of Widmanstätten α platelets produced higher peak stress than an alloy with globular primary α. However, it is seen in Fig. 3 that the initial microstructure has a negligible influence on the flow stress at steady state. The steady stress values of both material conditions are similar, perhaps indicating that similar microstructure characteristics have been generated in the material. As described above, the flow stress is sensitive to the initial microstructure, deformation temperature and strain rate.

3.2 Strain rate sensitivity

The strain rate sensitivity is usually used to determine the deformation mechanisms of a material. Values of the strain rate sensitivity (m) are calculated using the following expression [14]:

$$m=\left.\frac{\mathrm{d}\lg\sigma}{\mathrm{d}\lg\dot{\varepsilon}}\right|_{\varepsilon,T} \tag{1}$$

where σ is the flow stress at fixed strain and deformation temperature, $\dot{\varepsilon}$ is the strain rate, ε is the strain, and T is the thermodynamic deformation temperature.

The strain rate sensitivities of both material conditions are estimated from the flow stress−strain curves during isothermal compression of Ti−5Al−2Sn−2Zr−4Mo−4Cr alloy and are shown in Fig. 4. The values of strain rate sensitivity reveal a noticeable dependence on initial microstructure, deformation temperature and strain rate.

It is observed in Fig. 4(c) that m of microstructure AB is larger than that of microstructure B at a strain of 0.5, a strain rate of 0.01 s^{-1} and in the lower deformation temperature range of 770−830 °C, but at higher deformation temperatures (i.e., 850 °C, 870 °C), m of microstructure B is found to be larger. In the strain rate range of 0.1−1.0 s^{-1}, m of microstructure B is larger than or similar to that of microstructure AB at all given deformation temperatures. Similarly, m of microstructure AB is larger than that of microstructure B at a strain of 0.7, a strain rate of 0.01 s^{-1} and in the lower deformation temperature range of 770−810 °C, but m of microstructure B is larger than or near to that of microstructure AB at other processing parameters, as illustrated in Fig. 4(d). This phenomenon can be reasonably based on the microstructure evolution. Figures 4(a) and (e) show the microstructures of the alloy with different initial microstructures at a deformation

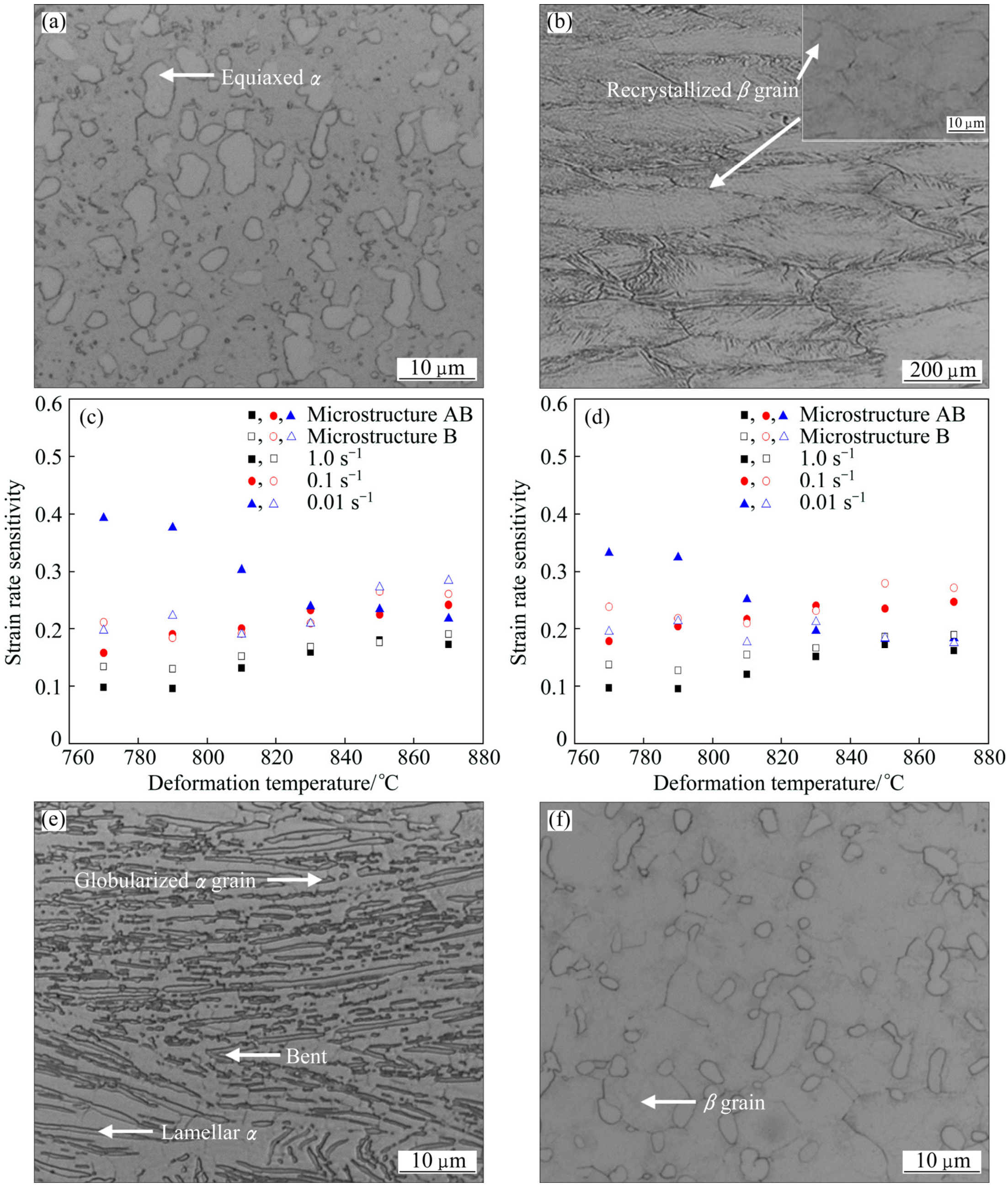

Fig. 4 Variations of strain rate sensitivity for Ti−5Al−2Sn−2Zr−4Mo−4Cr alloy with microstructures AB and B as function of deformation temperature and strain rate at strains of 0.5 (c) and 0.7 (d) with optical micrographs: (a) t=810 °C, $\dot{\varepsilon}$=0.01 s^{-1}, ε=0.5 (microstructure AB); (b) t=850 °C, $\dot{\varepsilon}$=0.01 s^{-1}, ε=0.5 (microstructure B); (e) t=810 °C, $\dot{\varepsilon}$=0.01 s^{-1}, ε=0.5 (microstructure B); (f) t=810 °C, $\dot{\varepsilon}$=0.01 s^{-1}, ε=0.5 (microstructure AB)

temperature of 810 °C, a strain rate of 0.01 s^{-1} and a strain of 0.5. It is observed in Fig. 4(a) that the α grains are equiaxed and fine, which are beneficial for grain boundary sliding and accommodation, but the microstructure in Fig. 4(e) is comprised of the lamellar α structure and a small amount of bent and kinked lamellae and globularized α. The α plates in microstructure B constrain the deformation of the soft β phase and are not beneficial for grain boundary sliding. Thus, m of microstructure AB is larger than that of microstructure B at the lower deformation temperature and strain rate. When the deformation temperature increases to 850 °C, equiaxed α phase in microstructure AB decreases to 11% and the β grains quickly grow up (Fig. 4(f)), which leads to a drop of m. However, lamellar α in microstructure B significantly decreases and dynamic recrystallization of β phase occurs in prior-β grain with increasing deformation temperature, which promotes an increase of m (Fig. 4(b)). So, m of microstructure B is larger at higher deformation temperatures (i.e., 850 °C, 870 °C).

In addition, it is also observed in Fig. 4 that the processing parameters have effects on m. For microstructure AB, m exceeds 0.30 at a strain of 0.5, a strain rate of 0.01 s^{-1} and in the deformation temperature range of 770−810 °C (Fig. 4(a)). This is most likely due to the occurrence of a grain boundary sliding mode of deformation, which is accommodated by matrix deformation [15]. The maximum m value of 0.39 occurs at a deformation temperature of 770 °C, indicating superplastic deformation behavior, the characteristic of which is well described in Ref. [10]. In the deformation temperature range of 830−870 °C, m falls into the range of 0.21−0.24, implying that the deformation mechanism is likely dislocation glide/climb. In the strain rate range of 0.1−1.0 s^{-1} and at all given deformation temperatures, Ti−5Al−2Sn−2Zr−4Mo−4Cr alloy with microstructure AB exhibits m values of approximately 0.20 or less. These m values imply that the deformation is controlled by dislocation glide, which is characteristic of power law creep [16,17].

For microstructure B, in the deformation temperature range of 850−870 °C and strain rate range of 0.01−0.1 s^{-1}, m falls into the range of 0.26−0.28, implying that the deformation mechanism is likely dislocation glide/climb. At other processing parameters, Ti−5Al−2Sn−2Zr−4Mo−4Cr alloy with microstructure B exhibits m values of approximately 0.20 or less, which are still typical of power law creep. According to above analysis, it is concluded that the initial microstructure, deformation temperature and strain rate have a significant effect on m.

3.3 Strain hardening exponent

The strain hardening exponent results from a balance between the strain hardening and softening mechanisms. In this study, the strain hardening exponent (n) is determined using the following expression:

$$n=\left.\frac{\mathrm{d}\lg\sigma}{\mathrm{d}\lg\varepsilon}\right|_{\dot{\varepsilon},T} \tag{2}$$

The strain hardening exponent of both material conditions is estimated from the flow stress−strain curves during isothermal compression and is shown in Fig. 5. From Fig. 5(a), it is shown that n of both material

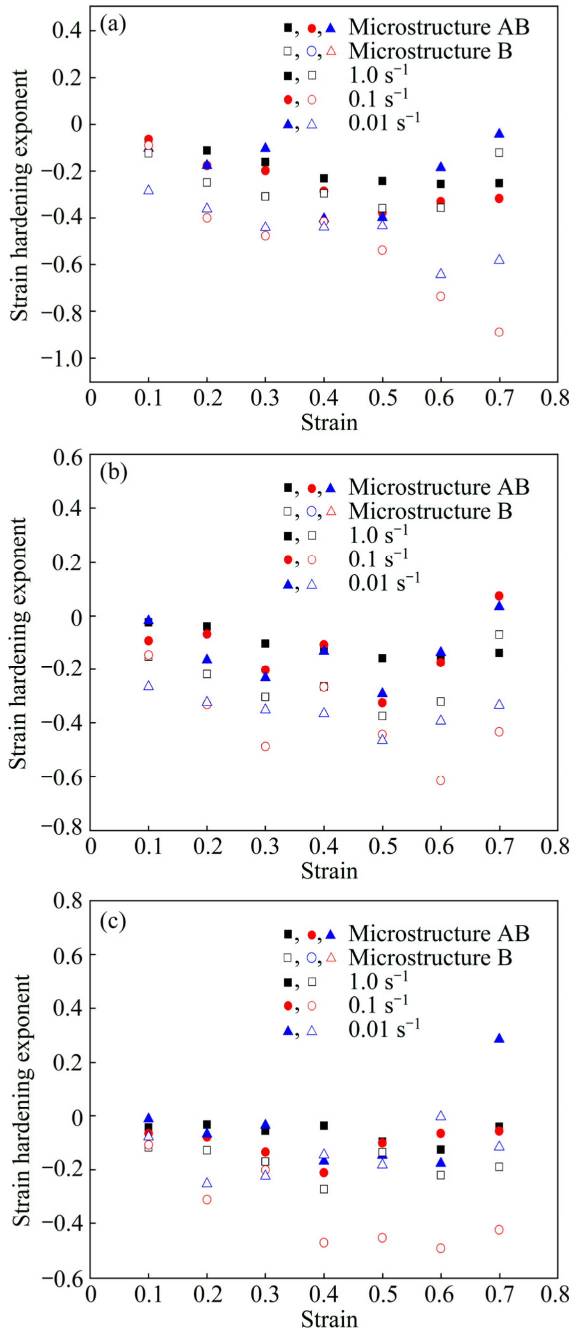

Fig. 5 Variations of strain hardening exponent for Ti−5Al−2Sn−2Zr−4Mo−4Cr alloy with microstructures AB and B as function of strain rate and strain at deformation temperatures of 770 °C (a), 810 °C (b) and 850 °C (c)

conditions is negative for the three tested strain rates at a deformation temperature of 770 °C. It is well known that the strain hardening exponent results from a competition between flow softening and strain hardening. The negative n values imply that the flow softening effect is predominant in the strain range of 0.1−0.7 for the three tested strain rates at a deformation temperature of 770 °C. It is also shown in Fig. 5(a) that n of microstructure AB is larger than that of microstructure B at a deformation temperature of 770 °C. This demonstrates that the flow softening effect of microstructure B is more significant than that of microstructure AB. The shapes of the flow curves during isothermal compression of the alloy are in support of this phenomenon (Fig. 3(a)). Similarly, JACKSON et al [6] noted that Ti−10V−2Fe−3Al alloy with a high aspect ratio of Widmanstätten α platelets produced higher flow softening than that with globular primary α.

At a deformation temperature of 810 °C (Fig. 5(b)), n of microstructure AB becomes positive at a strain of 0.7 in the strain rate range of 0.1−0.01 s^{-1}, which implies that the strain hardening plays a dominant role in the domain. However, n of both material conditions is negative at other processing parameters. At a deformation temperature of 850 °C (Fig. 5(c)), n of microstructure AB is positive at a strain of 0.7 and a strain rate of 0.01 s^{-1}.

In addition, it is also observed in Fig. 5 that the strain has a significant effect on n of microstructure B, but only a slight effect on n of microstructure AB. Detailed microstructure observations are required to explain this difference. Figures 6 and 7 show the effects of strain on microstructures AB and B at a deformation temperature of 810 °C and a strain rate of 1.0 s^{-1}, respectively. Figure 6 shows that strain has a slight effect on the morphology of the primary α phase. The microstructure has slightly oriented characteristics with increasing strain, and the grain size of the primary α phase decreases slightly when the strain increases from 0.5 to 0.9. However, it is observed in Fig. 7 that strain has a significant effect on the lamellar α structure. At a strain of 0.5, the microstructure consists of the lamellar α structure where a large fraction of the lamellae have rotated to be perpendicular to the compression axis (Fig. 7(a)). When the strain rises to 0.7, the microstructure is composed of bent and kinked lamellae and a small amount of globularized α phases (Fig. 7(b)). At a strain of 0.9, the microstructure is comprised of the almost fully equiaxed microstructure with a small amount of unglobularized lamellar α phases, as illustrated in Fig. 7(c). Therefore, platelet bending/kinking and dynamic globularization of α phase in microstructure B result in significant change in n with increasing strain. Similarly, SEMIATIN et al [18] proposed that the flow softening of the lamellar α structure can be attributed to platelet bending/kinking.

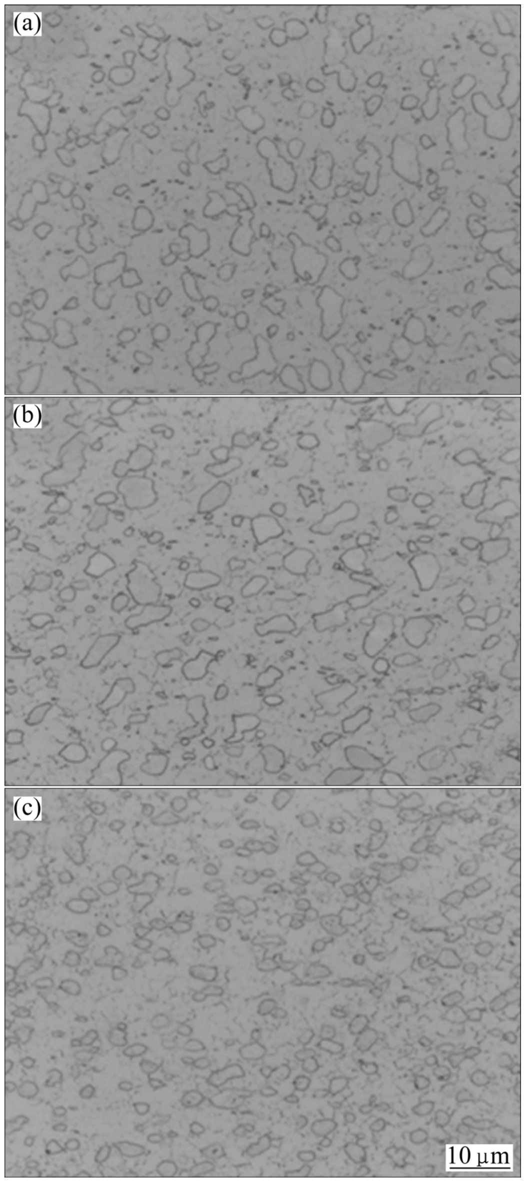

Fig. 6 Effect of strain on microstructure AB at deformation temperature of 810 °C and strain rate of 1.0 s^{-1} (OM): (a) 0.5; (b) 0.7; (c) 0.9

Similarly, the strain rate also has a significant effect on n of microstructure B, but only a slight effect on n of microstructure AB. This phenomenon is also attributed to the significant microstructure change of the alloy with microstructure B as the strain rate increases. According to the above analysis, it is concluded that the initial microstructure morphology has a significant effect on the strain hardening exponent during isothermal compression of Ti−5Al−2Sn−2Zr−4Mo−4Cr alloy. Additionally, the effect of strain and strain rate on the strain hardening exponent is dependent on the initial microstructure.

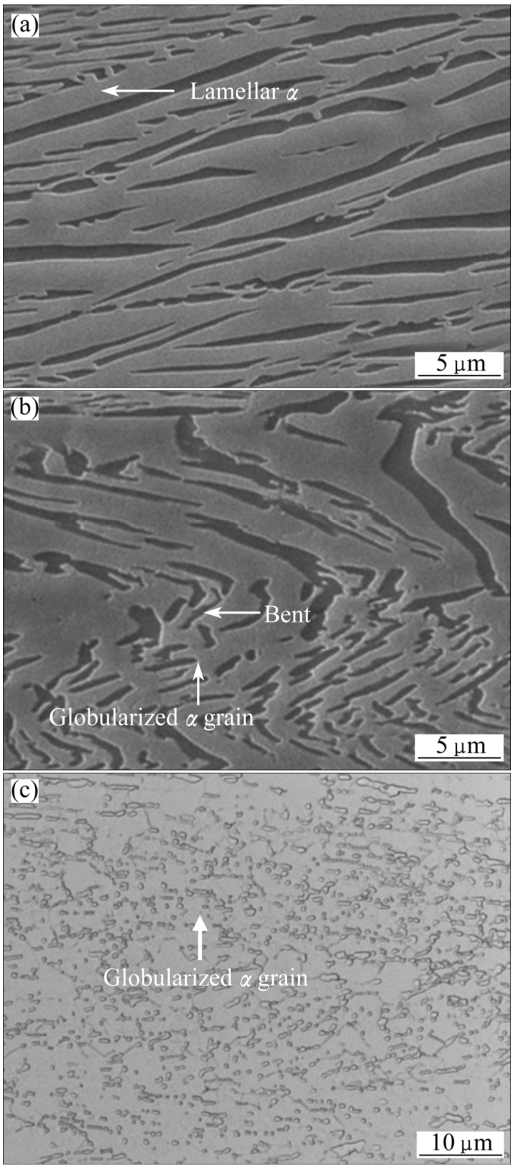

Fig. 7 Effect of strain on microstructure B at deformation temperature of 810 °C and strain rate of 1.0 s^{-1}: (a) 0.5; (b) 0.7 (SEM); (c) 0.9 (OM)

3.4 Apparent activation energy for deformation

The apparent activation energy for deformation describes the activation barrier that a transition of an atom is required to overcome, and it can be assumed to describe the workability of an alloy. Dependence of the flow stress on the deformation temperature and the strain rate at high temperature deformation is generally expressed in terms of a kinetic equation:

$$\dot{\varepsilon} = A\sigma^{1/m} \exp[-Q/(RT)] \tag{3}$$

From Eq. (3), the Q value at a given strain rate could be obtained as follows:

$$Q = \frac{R}{m}\frac{\partial \ln \sigma}{\partial (1/T)}\Big|_{\dot{\varepsilon}} \approx \frac{R}{m}\frac{\Delta \ln \sigma}{\Delta (1/T)}\Big|_{\dot{\varepsilon}} \tag{4}$$

m can be calculated in Eq. (1). With the help of the flow stress−strain curves during isothermal compression of Ti−5Al−2Sn−2Zr−4Mo−4Cr alloy and combining Eqs. (1) and (4), the apparent activation energy for deformation can be calculated for different initial microstructures and strains. The effect of initial microstructure and strain on the apparent activation energy for deformation of the alloy is shown in Fig. 8.

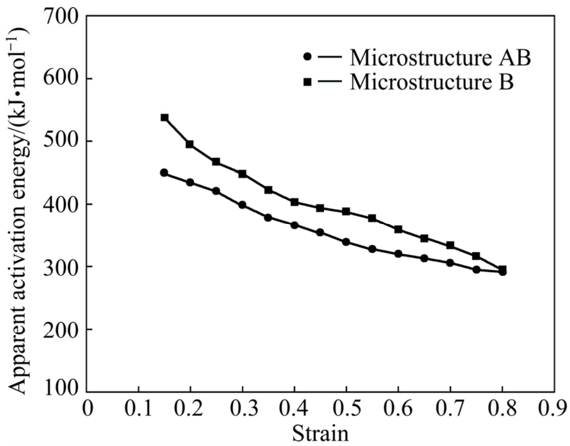

Fig. 8 Effect of initial microstructure and strain on apparent activation energy for deformation

From Fig. 8, it is observed that the initial microstructure significantly affects Q in the strain range of 0.15−0.55. At a strain of 0.15, Q of microstructure B is equal to 537.28 kJ/mol, which is higher than that of microstructure AB, which is equal to 449.56 kJ/mol. In the strain range of 0.6−0.8, the effect of initial microstructure on Q is small. When the strain reaches 0.8, Q of microstructure B is equal to 294.37 kJ/mol, which is similar to that of microstructure AB, which is 290.98 kJ/mol. This phenomenon can be reasonably explained based on the microstructure evolution of the alloy during isothermal compression. Early in the deformation, α phase in microstructure B always remains the lamellar structure where a large fraction of the lamellae have rotated to be perpendicular to the compression axis, as illustrated in Fig. 7(a). Widmanstätten α plates and grain boundary α constrain the deformation of the soft β phase; and the alloy with microstructure B has more grain boundaries than that with microstructure AB; grain boundaries act as obstacles to dislocation motion, leading to larger Q of microstructure B during early deformation. In later deformation, bulking of lamellar α and dynamic globularization in microstructure B occur, as shown in Fig. 7(b). This leads to the decrease of Q of microstructure B. The rate of dynamic globularization increases with increasing strain. When the strain reaches 0.8, possible similar microstructure characteristics (i.e., equiaxed and fine α phase) finally lead to the similar Q values in both material conditions. This phenomenon could be supported by the shapes of the flow stress−strain curves (Fig. 3). It is also shown in Fig. 8 that Q of both material conditions decreases with increasing strain, while the rate of decrease in microstructure B is larger. This indicates that the softening effect is important in the strain range of 0.15−0.8 and the softening effect of microstructure B is more significant than that of microstructure AB. According to the above analysis, it is concluded that the initial microstructure and strain have effects on the apparent activation energy for deformation of the alloy during isothermal compression.

4 Conclusions

1) The alloy with Widmanstätten α plates shows higher peak stress and flow softening than that with equiaxed primary α phase. The steady stress values of both material conditions are similar.

2) In the strain range of 0.5−0.7, m of the alloy with equiaxed primary α is larger at 0.01 s^{-1} and lower deformation temperatures. However, m of the alloy with Widmanstätten α plates is larger than or similar to that of equiaxed primary α when considering other tested processing parameters.

3) The initial microstructure has a significant effect on the strain hardening exponent of the alloy, and the effect of strain and strain rate on the strain hardening exponent is dependent on the initial microstructure.

4) Q of the alloy with Widmanstätten α plates is larger than or similar to that of equiaxed primary α. Q also decreases with increasing strain, while the decrease rate of the alloy with Widmanstätten α plates is also more acute.

References

[1] SHI Zhi-feng, GUO Hong-zhen, LIU Rui, WANG Xiao-chen, YAO Ze-kun. Microstructure and mechanical properties of TC21 titanium alloy by near-isothermal forging [J]. Transactions of Nonferrous Metals Society of China, 2015, 25(1): 72−79.

[2] PILEHVA F, ZAREI-HANZAKI A, FATEMI-VARZANEH S M. The influence of initial microstructure and temperature on the deformation behavior of AZ91 magnesium alloy [J]. Materials and Design, 2012, 42: 411−417.

[3] ZHANG Jing, CHEN Bo-quan, ZHANG Bao-xiang. Effect of initial microstructure on the hot compression deformation behavior of a 2219 aluminum alloy [J]. Materials and Design, 2012, 34: 15−21.

[4] ZHAO Xin, YANG Xiao-ling, JING Tian-fu. Effect of initial microstructure on warm deformation behavior of 45 steel [J]. Journal of Iron and Steel Research, 2012, 19(8): 75−78.

[5] ROBERTSON D G, MCSHANE H B. Isothermal hot deformation behavior of metastable β titanium alloy Ti−10V−2Fe−3Al [J]. Materials Science and Technology, 1997, 13: 575−583.

[6] JACKSON M, JONES N G, DYE D, DASHWOOD R J. Effect of initial microstructure on plastic flow behavior during isothermal forging of Ti−10V−2Fe−3Al [J]. Materials Science and Engineering A, 2009, 501: 248−254.

[7] MARTIN G, NAŹE L, CAILLETAUD G. Numerical multi-scale simulations of the mechanical behavior of β-metastable titanium alloys Ti5553 and Ti17 [J]. Procedia Engineering, 2011, 10: 1803−1808.

[8] LIU Jiang-lin, ZENG Wei-dong, LAI Yun-jin, JIA Zhi-qiang. Constitutive model of Ti17 titanium alloy with lamellar-type initial microstructure during hot deformation based on orthogonal analysis [J]. Materials Science and Engineering A, 2014, 597: 387−394.

[9] LI Hong, ZHANG Chao, LIU Hong-bin, LI Miao-quan. Bonding interface characteristic and shear strength of diffusion bonded of Ti-17 titanium alloy [J]. Transactions of Nonferrous Metals Society of China, 2015, 25(1): 80−87.

[10] LUO Jiao, LI Liang, LI Miao-quan. The flow behavior and processing maps during the isothermal compression of Ti17 alloy [J]. Materials Science and Engineering A, 2014, 606: 165−174.

[11] LI L, LIM Q, LUO J. Flows softening mechanism of Ti−5Al−2Sn−2Zr−4Mo−4Cr with different initial microstructures at elevated temperature deformation [J]. Materials Science and Engineering A, 2015, 628: 11−20.

[12] WANJARA P, JAHAZI M, MONAJATI H, YUE S, IMMARIGEON J P. Hot working behavior of near-α alloy IMI834 [J]. Materials Science and Engineering A, 2005, 396: 50−60.

[13] WEISS I, SEMIATIN S L. Thermomechanical processing of alpha titanium alloys-an overview [J]. Materials Science and Engineering A, 1999, 263: 243−256.

[14] LUO Jiao, LI Miao-quan, YU Wei-xin, LI Hong. The variation of strain rate sensitivity exponent and strain hardening exponent in isothermal compression of Ti−6Al−4V alloy [J]. Materials and Design, 2010, 31: 741−748.

[15] KIM J H, SEMIATIN S L, LEE C S. High temperature deformation and grain boundary characteristics of titanium alloys with an equiaxed microstructure [J]. Materials Science and Engineering A, 2008, 485: 601−612.

[16] COURTNEY T H. Mechanical behavior of materials [M]. New York: McGraw Hill, 1990.

[17] FROST H J, ASHBY M J. Deformation mechanism maps [M]. Oxford, UK: Pergamon Press, 1982.

[18] SEMIATIN S L, SEETHARAMAN V, WEISS I. Flow behavior and globularization kinetics during hot working of Ti−6Al−4V with a colony alpha microstructure [J]. Materials Science and Engineering A, 1999, 263: 257−271.

热加工过程中 2 种原始组织的 Ti−5Al−2Sn−2Zr−4Mo−4Cr 合金变形行为

罗 皎，李 莲，李淼泉

西北工业大学 材料学院，西安 710072

摘 要：采用等温压缩试验研究不同原始组织对 Ti−5Al−2Sn−2Zr−4Mo−4Cr 合金流动应力、应变速率敏感性指数、应变硬化指数和表观变形激活能的影响。结果表明：原始组织为片层组织的 Ti−5Al−2Sn−2Zr−4Mo−4Cr 合金具有更高的峰值应力和流动软化效应，当变形温度高于或等于 810 °C、应变速率为 0.1~5.0 s^{-1} 时，原始组织为等轴组织的 Ti−5Al−2Sn−2Zr−4Mo−4Cr 合金存在初始屈服现象。当应变为 0.5~0.7、变形温度较低、应变速率为 0.01 s^{-1} 时，原始组织为等轴组织的 Ti−5Al−2Sn−2Zr−4Mo−4Cr 合金的应变速率敏感性指数值较大，这主要归因于其显微组织演变特征。随着变形的进行，原始组织为片层组织的 Ti−5Al−2Sn−2Zr−4Mo−4Cr 合金发生了 α 片层弯曲和动态球化现象，这使得其应变硬化指数变化显著。当应变为 0.15~0.55 时，原始组织为片层组织的 Ti−5Al−2Sn−2Zr−4Mo−4Cr 合金的表观变形激活能更大。

关键词：钛合金；等温压缩；流动应力；显微组织演变；动态球化

(Edited by Xiang-qun LI)